Acta Cryst. (1996). B52, 314–322

Structure of Vanadocene in the Temperature Interval 108–357 K and the Nature of the Ring Disorder

M. Yu. Antipin[a] and R. Boese[b]

[a]*Institute of Organoelement Compounds, Russian Academy of Sciences (INEOS), Vavilov Str. 28, Moscow B-334, Russia, and* [b]*Institüt für Anorganische Chemie der Universität-GH Essen, Universitätstrasse 5-7, D-45117 Essen, Germany*

(*Received 7 November 1994; accepted 1 September 1995*)

Abstract

The crystal structure of vanadocene, bis(η^5-2,4-cyclopentadien-1-yl)vanadium, Cp_2V, has been studied at the four temperatures 108, 170, 297 and 357 K by X-ray diffraction in order to elucidate the nature of the Cp-ring disorder and compare the results obtained with similar data for formally isostructural ferrocene, cobaltocene and nickelocene. A careful analysis of the anisotropic displacement parameters (ADP's) for Cp_2V showed that at 108 K the crystal structure is ordered (staggered Cp_2V molecules occupy centres of symmetry in the space group $P2_1/n$, $Z = 2$), which distinguishes vanadocene from its formal analogues and some Cp-ring disorder starts at *ca* 170 K. A model of this disorder has been proposed with two distinct orientations of the ring, differing in temperature-dependent occupancy factors and by a rotation in the ring plane of almost 36°. The fractional contributions of the second (minor) ring orientation are 0.05, 0.17 and 0.35, respectively, at 170, 297 and 357 K. The energetic characteristics of the ring rotation motion in the Cp_2V crystal were estimated from ADP analysis and compared with similar data for other 3*d*-metallocenes.

1. Introduction

Vanadocene, Cp_2V, belongs to the well known series of the sandwich-like metal π-complexes Cp_2M, where M = 3*d*- (or 4*d*-) transition metals and Cp is the C_5H_5 ligand. The most studied 3*d*-metallocene is ferrocene, Cp_2Fe, which has more than a 40-year history of structural investigations. The sandwich-like structure of Cp_2Fe was first demonstrated by X-ray analysis using projection methods as early as 1952–1953 by Fischer & Pfab (1952), Eiland & Pepinsky (1952) and Dunitz & Orgel (1953), almost immediately after the first publications (Kealy & Pauson, 1951; Miller, Tebboth & Tremaine, 1952; Wilkinson, Rosenblum, Whiting & Woodward, 1952) describing the synthesis and making suggestions about its unusual structure.

The first three-dimensional X-ray structure of ferrocene was published by Dunitz, Orgel & Rich (1956). A staggered conformation, required by the position of the metal at a centre of symmetry ($P2_1/a$, $Z = 2$), was found for this molecule and rotation oscillations of the Cp ring about its mean position in the crystal were suggested. Around the same time crystals of cobaltocene, nickelocene (Pfab & Fischer, 1953) and vanadocene (Weiss & Fischer, 1955) were found to be isomorphous to ferrocene at room temperature. Due to the similarity of these isomorphous compounds it was assumed for a long time that Cp_2Co, Cp_2Ni and Cp_2V have the same crystal structure as Cp_2Fe and, therefore, the structure of ferrocene as a typical representative of the 3*d*-metallocene series was studied more carefully using different methods: X-ray analysis (Seiler & Dunitz, 1979*a*,*b*; Calvarin, Clec'h, Berar & Andre, 1982; Calvarin, Berar & Clec'h, 1982), neutron diffraction (Willis, 1960; Takusagawa & Koetzle, 1979), theoretical calculations of the crystal packing (Calvarin, Berar & Clec'h, 1982), spin-lattice NMR relaxation (Campbell, Fyfe, Harold-Smith & Jeffrey, 1976) *etc.* It should be noted that at room temperature crystals of some other metallocenes, namely Cp_2Mg (Bünder & Weiss, 1975*a*) and Cp_2Be (Wong, Lee, Chao & Lee, 1972), are also isomorphous with the monoclinic ferrocene.

However, other data for the 3*d*-metallocenes considered showed that despite the formal similarity of their crystal structures there are some important differences in this series. Thus, it is well known that at 163.9 K ferrocene undergoes a distinct phase transition (Edwards, Kington & Mason, 1960) between the disordered room-temperature monoclinic phase and an ordered low-temperature triclinic one. On the contrary, no sharp phase transitions were detected for the monoclinic analogues of ferrocene (Cp_2Co, Cp_2Ni and Cp_2V). Moreover, a new thermodynamically stable, up to 242 K, orthorhombic modification (space group *Pnma*, $Z = 4$) was also studied for ferrocene at 98 K by Seiler & Dunitz (1982) and it was established that this phase is isomorphous with that for ruthenocene, studied at 100 and 293 K (Seiler & Dunitz, 1980*b*). It is clear, therefore, that the analogy of 3*d*-metallocene compounds with ferrocene cannot be pressed too far because of their different thermal behaviour.

Detailed analyses of monoclinic and triclinic modifications of Cp_2Fe (room-temperature phase at 173 and 293 K, low-temperature phase at 101, 123 and 148 K)

and their relationships were established by Seiler & Dunitz (1979*a*,*b*). In accordance with their data in the triclinic low-temperature phase there are two independent Cp_2Fe molecules with D_5 symmetry, the rings being rotated by approximately 9° from the eclipsed conformation. In the disordered monoclinic room-temperature phase the asymmetric unit contains only one independent Cp ring that may be regarded as a superposition of the four independent rings of the low-temperature phase. The molecular centre of symmetry required by the space group $P2_1/a$ ($Z = 2$) is statistical and the nature of the disorder is static: the shape and dimensions of the Cp-ring thermal ellipsoids in the room-temperature phase at 173 and 293 K are almost temperature-independent.

The structure of the monoclinic modification of nickelocene was made at 293 and 101 K (Seiler & Dunitz, 1980*a*). At room temperature the marked similarity between the thermal ellipsoid pattern for Cp_2Ni and the room-temperature phase of Cp_2Fe suggested the same nature of disorder for these compounds. For example, the molecular libration amplitude $\mathbf{L}_1$ about the fivefold axis in Cp_2Ni at 293 K is abnormally large (199 deg^2) and close to that of ferrocene at the same temperature: 258 deg^2 from neutron diffraction data (Takusagawa & Koetzle, 1979) and 220 deg^2 from the X-ray study (Seiler & Dunitz, 1979*b*). The same pattern was also observed for room-temperature structures of Cp_2Co and Cp_2V (see below). On cooling the nickelocene crystal to 101 K, a decrease of the displacement parameters occurs and their values at low temperature are quite normal. This means that some dynamic ordering occurs in the crystal, but no model of this process was suggested. It is interesting to note that in the incoherent quasielastic neutron scattering (IQENS) spectra of Cp_2Ni some features near 200 K were detected that were attributed to a weak order–disorder transition in this compound (Sourisseau, Lucazeau, Dianoux & Poinsignon, 1983).

The crystal structure of Cp_2Co at room temperature was first determined by Bünder & Weiss (1975*b*), but no analysis of atomic thermal ellipsoids or discussion of the possible disorder in the crystal was made. This structure was redetermined by the authors of the present paper (Antipin, Boese, Augart & Schmidt, 1993), using two new X-ray data sets at 100 and 297 K, and in this paper a careful analysis of the molecular geometry, crystal packing and atomic displacement parameters was performed. It was found that the room-temperature structure of Cp_2Co is disordered, as are ferrocene and nickelocene. An atomic model of this disorder was suggested with two distinct orientations of the Cp ring, differing in occupancy factors (80 and 20%) and by a rotation angle in the ring plane of approximately 34°. An ordering of the Cp-ring position was observed at 100 K with the second minor orientation contribution decreasing to *ca* 10%. Thus, the disorder in Cp_2Co is dynamic (temperature-dependent), but no detectable phase transition was noted for this compound (Azokpota, Pommier, Berar & Calvarin, 1977). The gradual appearance in the crystal of the second ring orientation upon increasing the temperature may correspond to the appearance of almost eclipsed molecules, if the molecular centre of symmetry is considered to be statistical in nature, as was suggested for room-temperature phases of Cp_2Fe and Cp_2Ni.

The first crystal structure determination of vanadocene at room temperature was made by Antipin, Lobkovskii, Semenenko, Soloveitchik & Struchkov (1979). The molecular structure was found to be centrosymmetric ($P2_1/n$, $Z = 2$, $R = 0.048$ for 588 reflections) with mean V—C distance 2.25 (1) Å and V-ring centre distance 1.920 Å. A libration of the Cp ring was noted. This structure was redetermined later by Rogers, Atwood, Foust & Rausch (1981) at room temperature (583 reflections, $R = 0.031$), with a more detailed analysis of the ring disorder. A difference-Fourier map in the ring plane revealed five new peaks with maxima located approximately midway between the C atoms of the main frame, thus indicating a second ring orientation. From the peak heights the occupancy factors were initially assumed to be 0.67 and 0.33 and the final refinement converged with the occupancy coefficient ratio 0.70:0.30 for main and minor orientations.

Thus, the thermal behaviour of the Cp rings in crystals of Cp_2Ni, Cp_2Co and Cp_2V is apparently very similar, but multi-temperature X-ray diffraction data in the large temperature interval are absent for this series. Such data may provide important information about Cp ring motion and the nature of disorder. In order to clarify this question in the present paper we have studied the crystal structure of vanadocene at four temperatures: 108, 170, 297 and 357 K.

2. Experimental

All experimental data were obtained for one single crystal of vanadocene with the dimensions *ca* 0.3 × 0.3 × 0.3 mm using a Nicolet *R3m/V* diffractometer (monochromatized Mo $K\alpha$ radiation, $\lambda = 0.7107$ Å), first at 108 K and then at 170, 297 and 357 K. Unit-cell parameters were refined using 25 reflections with 2θ = 20–25° and these parameters are given in Table 1. All reflections were measured using the Wyckoff-type scan method with the scan range 0.9° in the interval $2\theta \le 90°$ at 108 K (full sphere), $2\theta \le 60°$ at 170 and 297 K (half sphere) and $2\theta \le 60°$ at 357 K (asymmetric unit of reciprocal space), see Table 2. The agreement between intensities of equivalent reflections (R_{int}) was equal to 0.024–0.025. A relatively small number of reflections was measured at 357 K due to crystal decomposition at this temperature. An empirical absorption correction was applied for data sets at 108, 170 and 297 K using the standard psi-scan method (for data at 108 K the max/min transmission coefficients were found to be

0.95/0.82 with R_{merg} = 0.023 and 0.015 before and after correction).

As cited above and in the previous X-ray structural studies of vanadocene and cobaltocene, the same setting of the space group $P2_1/n$ was chosen for vanadocene in the present work, mainly for a more convenient comparison between Cp_2V and Cp_2Co structures, where essentially the same nature of the ring disorder takes place. This setting differs from that assumed traditionally for ferrocene and nickelocene ($P2_1/a$ setting). Nevertheless, this type of space-group transformation will not affect the structural parameters discussed here for the 3*d*-metallocene series, including the cell parameter *b*, having unusual temperature dependence.

As may be seen from Table 1, the temperature dependence of the cell parameter *b* on cooling is abnormal: while *a* and *c* and the unit-cell volume decrease normally on cooling, the *b* parameter increases, thus having a negative thermal expansion coefficient. It is important to note that virtually the same behaviour was observed earlier for nickelocene, namely negative thermal expansion of the *b* axis in the interval 100–293 K (Seiler & Dunitz, 1980*a*) and cobaltocene (Antipin, Boese, Augart & Schmidt, 1993), where the value of the *b* axis is almost temperature independent in the interval 120–300 K with a small negative slope around 120 K, but not for the monoclinic modification of ferrocene in the interval 173–293 K (Seiler & Dunitz, 1979*a*). These results correlate well with the observation of a sharp phase transition only for ferrocene in the series considered and it was explained for Cp_2Fe, Cp_2Ni (Braga & Grepioni, 1992) and Cp_2Co (Antipin, Boese, Augart & Schmidt, 1993) on the basis of detailed analysis of the crystal packing in these compounds.

In order to check the thermal behaviour of solid vanadocene, a DSC thermogram of a powder sample of Cp_2V was recorded in the interval 100–300 K, with the temperature increasing at a rate of 10° min^{-1}. There was no distinct phase transition for this sample, but some small irregularities were detected on the DSC curve at *ca* 145 K and more markedly at 210–215 K, probably indicating the onset of some order–disorder process in the crystal. It should be noted that calorimetric data for solid vanadocene, reported in the review by Domalski & Hearing (1990), also give some evidence for a weak phase transition (probably of a λ-type) in this compound in the temperature interval 130–200 K.

2.1. *Refinement*

During refinement of the X-ray data for vanadocene in this study we used the same approach as in the above-mentioned analysis of the cobaltocene crystal structure at 100 and 297 K.

A conventional refinement (C model) of the data at 297 K led to rather high *R* values (*R* = 0.0456, *wR* = 0.0583, GOF = 1.592), very high anisotropic displacement parameters for the C atoms of the ring and a large scatter (δ) of the chemically equivalent C—C bond lengths [from 1.351 (6) to 1.433 (6) Å, δ = 0.082 Å]. H atoms in this refinement were fixed at ideal positions, but their isotropic thermal parameters were refined. As for cobaltocene at 100 and 297 K, and earlier for vanadocene (Rogers, Atwood, Foust & Rausch, 1981), analysis of the difference electron-density maps in the Cp-ring plane revealed additional maxima located in this plane and approximately midway between the C atoms of the main frame. These maxima were interpreted as corresponding to a second minor orientation of the ring, twisted by almost 30° with respect to the main frame and shifted from its centre (see below). This two-orientation (TO) model was refined for different values of occupancy factors and the best *R* values (*R* = 0.0338, *wR* = 0.0414, GOF = 1.146) at room temperature were obtained with this model for the ratio 0.83:0.17 for the main and minor orientation occupancy factors. During this refinement the C atoms of the second orientation of the ring were treated as a rigid group (but their isotropic thermal parameters were refined), with the H atoms attached to them at ideal positions.

Table 1. *Unit-cell parameters of the Cp_2V crystal at different temperatures*

T (K)	108	170	297	357
a (Å)	5.7208 (6)	5.772 (1)	5.885 (1)	5.934 (2)
b (Å)	8.211 (1)	8.111 (2)	8.013 (3)	8.013 (4)
c (Å)	8.831 (1)	8.981 (2)	9.251 (3)	9.344 (4)
β (°)	90.94 (1)	89.95 (2)	88.80 (2)	91.52 (4)
V (Å^3)	414.77 (9)	420.4 (2)	436.1 (2)	444.2 (5)

A conventional refinement of the data at 108 K converged to rather low *R* values (*R* = 0.0318, *wR* = 0.0376, GOF = 1.148), giving normal atomic displacement parameters for C atoms and more regular molecular geometry [C—C bond lengths 1.413 (1)–1.423 (1) Å, δ = 0.010 Å]. H-atom positions in this model were refined together with their isotropic temperature factors. No indication of the ring disorder was detected at this temperature and, therefore, the vanadocene structure at 108 K was assumed to be ordered.

On the other hand, at 170 K some residual disorder of the Cp ring is probably present in the crystal. This was suggested by the thermal ellipsoid shape and by subsequent analysis of the anisotropic displacement parameters. The TO model with the occupancy ratio 0.95:0.05 was found to be significant in this case. The Cp ring of the second orientation at 170 K was refined as a rigid group and because of the very low occupancy factor for this minor orientation, the corresponding isotropic thermal parameters of the C atoms were fixed at 0.06 Å^2. For both TO and C models at 170 K, as well as for data at 297 K, H atoms of the main orientation were fixed at ideal positions, but their isotropic thermal parameters were refined.

Table 2. *Results of refinement for the Cp_2V structure (C = conventional model, TO = two-orientation model; relative occupancies are given in parentheses)*

T (K)	108	170		297		357
Model	C	C	TO	C	TO	TO
	—	—	(0.95/0.05)	—	(0.83/0.17)	(0.65/0.35)
N_{tot}	7105	2973	2973	2677	2677	1500
N_{ref} ($\|F\| > 4\sigma$)	2783	1216	1216	950	950	442
N_{par}	72	57	60	57	65	35
R	0.0318	0.0378	0.0359	0.0456	0.0338	0.1302
wR	0.0376	0.0474	0.0448	0.0583	0.0414	0.1168
GOF	1.148	1.340	1.283	1.592	1.146	2.512

Calculations were made on a MicroVAXII computer using the *SHELXTL-Plus* (Sheldrick, 1991) program. For rigid Cp cycles of the second orientation (TO models) the C—C distances were taken as 1.420 Å, bond angles 108° and C—H bond lengths were fixed at 0.96 Å. Atomic scattering factors were taken from Cromer & Mann (1968).

The data at 357 K were refined only in the TO-model approximation. Refinement with the conventional model resulted in unrealistic molecular geometry and very high R values. Due to the relatively bad quality of the diffraction data obtained at this temperature and the small number of observed reflections, all C atoms were refined isotropically (atoms of the main frame were refined independently, while those of the minor orientation were treated as a rigid group, but their isotropic thermal parameters were refined). H-atom positions and their thermal parameters for both orientations were fixed. The best result was obtained for the occupancy ratio 0.65:0.35 with the expected molecular geometry for the main orientation [C—C bond lengths in the interval 1.39 (3)–1.44 (3) Å]. A model with two distinct rigid-body rings having different occupancy factors was also tested and resulted in very similar occupancies.

Refinement results are summarized in Table 2. Atomic coordinates and anisotropic displacement parameters [calculated using the weighting scheme of Dunitz & Seiler (1973) with B = 5.0] are given in Tables 3 and 4. H-atom coordinates for data at 108 K are presented in Table 5.* A thermal ellipsoid representation of the Cp rings at different temperatures for both models is shown in Fig. 1.

3. Results and discussion

3.1. *Molecular geometry and crystal packing*

The best results for Cp_2V molecular geometry were obtained with the data at 108 K (Table 6). The V—C bond lengths are equal to 2.260 (1)–2.278 (1) Å (mean value 2.269 Å) and C—C 1.413 (1)–1.423 (1) Å (mean value 1.417 Å). The Cp ring is planar within 0.001 Å and the distance from the metal atom to the ring centre is 1.923 Å. These values, especially after correction for libration, are close to those found for

Table 3. *Atomic coordinates ($\times 10^4$) and equivalent isotropic displacement factors ($Å^2 \times 10^4$) in Cp_2V crystal at 108, 170, 297 and 357 K*

	x	y	z	U_{eq}
V*	0	0	0	168 (1)
				267 (1)
				268 (1)
				503 (2)
				505 (1)
				654 (10)
C(1)	−2618 (1)	−735 (1)	1785 (1)	223 (2)
	−2624 (3)	−774 (2)	1741 (2)	377 (4)
	−2636 (3)	−772 (2)	1742 (2)	373 (4)
	−2610 (6)	−820 (4)	1679 (4)	770 (8)
	−2666 (4)	−820 (3)	1658 (3)	627 (6)
	−2581 (31)	−770 (29)	1701 (22)	759 (50)
C(2)	−2780 (1)	−1859 (1)	576 (1)	229 (2)
	−2771 (3)	−1868 (2)	548 (2)	379 (4)
	−2769 (3)	−1870 (2)	551 (2)	373 (4)
	−2737 (6)	−1864 (4)	538 (4)	745 (8)
	−2724 (5)	−1920 (4)	480 (3)	727 (6)
	−2827 (29)	−1849 (22)	546 (2)	627 (33)
C(3)	−600 (2)	−2669 (1)	481 (1)	268 (2)
	−657 (4)	−2696 (2)	426 (2)	468 (5)
	−650 (4)	−2694 (2)	435 (2)	449 (5)
	−738 (8)	−2704 (4)	379 (4)	898 (8)
	−634 (6)	−2719 (3)	420 (4)	824 (6)
	−755 (37)	−2741 (25)	251 (22)	723 (47)
C(4)	909 (2)	−2041 (1)	1636 (1)	285 (2)
	821 (3)	−2099 (3)	1567 (3)	524 (5)
	823 (3)	−2095 (3)	1575 (2)	490 (5)
	739 (6)	−2135 (5)	1488 (5)	988 (9)
	740 (5)	−2126 (3)	1517 (3)	786 (6)
	732 (35)	−2209 (26)	1333 (24)	694 (39)
C(5)	−353 (2)	−844 (1)	2443 (1)	253 (2)
	−429 (4)	−903 (2)	2374 (2)	440 (5)
	−438 (4)	−897 (2)	2378 (2)	415 (4)
	−527 (7)	−957 (4)	2281 (4)	853 (9)
	−531 (5)	−924 (3)	2305 (3)	680 (6)
	−330 (46)	−1013 (28)	2213 (27)	773 (46)
C(15)†	−2069 (16)	−851 (16)	1681 (15)	600
	−1650 (9)	−802 (7)	1969 (6)	545 (13)
	−1132 (54)	−780 (41)	2274 (33)	1027 (170)
C(12)	−2788	−1842	463	600
	−2774	−1609	819	437 (13)
	−2861	−1261	1337	896 (120)
C(23)	−877	−2827	15	600
	−1198	−2706	128	518 (14)
	−1952	−2465	365	953 (110)
C(34)	1024	−2444	956	600
	900	−2576	851	508 (13)
	340	−2728	706	675 (85)
C(45)	288	−1223	1986	600
	621	−1399	1988	582 (13)
	847	−1686	1884	530 (55)

* Data are given in the sequence: first line – at 108 K, second – conventional (C) model at 170 K, third – two-orientation (TO) model at 170 K; then C model at 297 K, TO model at 297 K and TO model at 357 K. † Atoms C(15)–C(45) belong to the second orientation of the rigid Cp ring; standard deviations are given only for the pivot atom. Data are given for TO models in the sequence 170, 297 and 357 K.

* A list of structure factors and a summary of experimental details have been deposited with the IUCr (Reference: BK0022). Copies may be obtained through The Managing Editor, International Union of Crystallography, 5 Abbey Square, Chester CH1 2HU, England.

Table 4. *Anisotropic atomic displacement factors ($Å^2 \times 10^4$) in Cp_2V at 108, 170 (C and TO models) and 297 K (C and TO models)*

	U_{11}	U_{22}	U_{33}	U_{23}	U_{13}	U_{12}
V	189 (1)	145 (1)	170 (1)	37 (1)	23 (1)	2 (1)
	294 (2)	230 (2)	278 (2)	70 (1)	26 (1)	−1 (1)
	296 (2)	230 (2)	279 (2)	70 (1)	26 (1)	−1 (1)
	564 (3)	420 (3)	521 (3)	102 (2)	48 (3)	−1 (2)
	565 (2)	422 (2)	525 (2)	103 (2)	47 (2)	−5 (2)
C(1)	253 (3)	226 (3)	192 (3)	14 (2)	64 (2)	23 (2)
	438 (8)	367 (7)	325 (7)	56 (6)	121 (6)	27 (7)
	410 (8)	360 (7)	315 (7)	58 (6)	123 (6)	30 (6)
	842 (15)	735 (15)	721 (14)	183 (12)	261 (13)	78 (14)
	606 (10)	676 (11)	593 (10)	156 (9)	156 (9)	29 (10)
C(2)	252 (3)	231 (3)	205 (3)	7 (2)	24 (2)	−61 (2)
	413 (8)	387 (7)	339 (7)	36 (6)	27 (6)	−137 (6)
	409 (8)	379 (7)	331 (7)	39 (6)	30 (6)	−142 (6)
	819 (14)	689 (13)	725 (14)	84 (12)	68 (13)	−196 (14)
	912 (12)	651 (11)	612 (10)	−28 (9)	105 (10)	−263 (10)
C(3)	383 (4)	149 (2)	278 (3)	26 (2)	122 (3)	18 (3)
	721 (11)	217 (6)	464 (8)	50 (6)	256 (8)	18 (7)
	710 (10)	206 (6)	432 (8)	43 (6)	244 (8)	15 (7)
	1432 (17)	387 (11)	854 (14)	57 (11)	465 (15)	−14 (14)
	1291 (13)	379 (7)	792 (11)	56 (9)	339 (11)	−27 (10)
C(4)	244 (3)	278 (3)	334 (4)	157 (3)	36 (3)	46 (3)
	368 (8)	511 (9)	693 (10)	385 (8)	63 (8)	67 (7)
	363 (8)	474 (8)	633 (10)	349 (8)	75 (7)	76 (7)
	645 (13)	959 (15)	1354 (17)	765 (14)	134 (14)	149 (13)
	757 (11)	700 (11)	900 (11)	426 (10)	188 (10)	179 (10)
C(5)	325 (4)	253 (3)	179 (3)	49 (2)	−26 (2)	−50 (3)
	622 (10)	414 (8)	283 (6)	109 (6)	−51 (7)	−124 (8)
	585 (9)	395 (7)	264 (6)	99 (6)	−40 (6)	−110 (7)
	1227 (17)	795 (15)	538 (12)	177 (12)	−60 (14)	−257 (15)
	846 (11)	719 (9)	479 (9)	148 (9)	−27 (9)	−107 (10)

Table 5. *H-atom coordinates ($\times 10^3$) and their isotropic atomic displacement factors ($Å^2 \times 10^3$) at 108 K*

	x	y	z	U
H(1)	−374 (5)	3 (2)	207 (3)	36 (6)
H(2)	−408 (4)	−204 (2)	−5 (2)	37 (4)
H(3)	−31 (3)	−348 (3)	−26 (2)	43 (5)
H(4)	245 (3)	−241 (3)	185 (2)	48 (5)
H(5)	18 (4)	−20 (2)	328 (3)	35 (5)

vanadocene in the gas phase using electron diffraction (ED): V—C 2.280 (5), C—C 1.434 (3), V-center of the ring 1.928 (6) Å (Gard, Haaland, Novak & Seip, 1975). It should be noted that the best agreement between calculated and experimental ED curves was obtained for the molecular model with eclipsed Cp rings (R = 0.129), but the staggered model also cannot be ruled out (R = 0.132). The C—H bond lengths are 0.94 (2)–0.96 (2) Å and the displacements of these atoms from the C-atom ring plane are small and hardly significant.

The molecular geometry obtained with data at higher temperatures is characterized by a larger scatter among the chemically equivalent C—C bond lengths in the ring. Thus, in the C-model approximation the values of δ at 170 and 297 K are 0.027 and 0.082 Å. The TO model gives better results, namely, at the same temperatures δ = 0.023 and 0.027 Å (at 357 K the value of δ is 0.050 Å). Such 'improvement' of the molecular geometry may be considered as an additional argument for the TO-model validity.

Table 6. *Molecular geometry of vanadocene at 108 K*

		Libration correction			Libration correction
V—C(1)	2.273 (1)	2.279	C(1)—C(2)	1.413 (1)	1.422
V—C(2)	2.268 (1)	2.270	C(2)—C(3)	1.417 (1)	1.427
V—C(3)	2.260 (1)	2.268	C(3)—C(4)	1.423 (1)	1.432
V—C(4)	2.267 (1)	2.275	C(4)—C(5)	1.418 (1)	1.427
V—C(5)	2.278 (1)	2.284	C(1)—C(5)	1.414 (1)	1.424
Mean	2.269	2.27		1.417	1.426

C(2)—C(1)—C(5)	108.5 (1)
C(1)—C(2)—C(3)	107.7 (1)
C(2)—C(3)—C(4)	108.1 (1)
C(3)—C(4)—C(5)	107.7 (1)
C(1)—C(5)—C(4)	108.0 (1)
Mean C—C—C	108.0

A schematic representation of two orientations of the Cp ring in Cp_2V at 170, 297 and 357 K is shown in Fig. 2. As in cobaltocene, the second ring (Cp*) is not only tilted with respect to the main orientation (the interplane angle Cp/Cp* is equal to 3.0, 4.0 and 3.4° at 170, 297 and 357 K), but it is also slipped from the Cp-ring centre. The distance between centroids of the Cp and Cp* rings is 0.35 Å at 170 K, 0.25 Å at 297 K and 0.17 Å at 357 K. The relatively large value of this distance at 170 K is hardly significant because of the very small

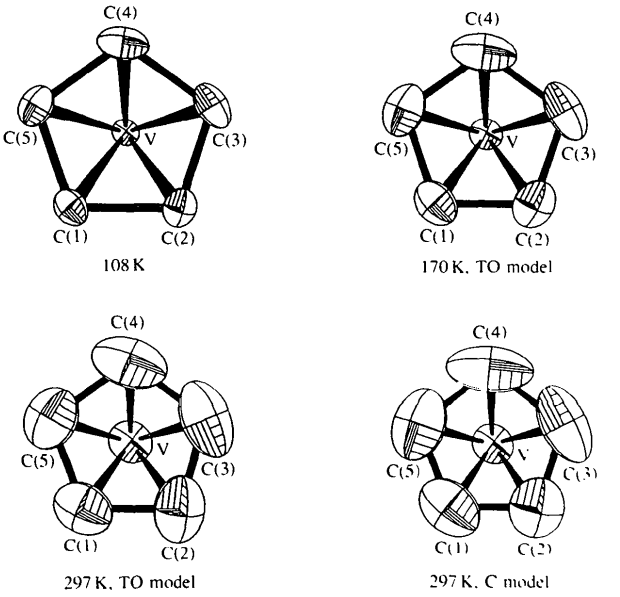

Fig. 1. Thermal ellipsoid (p = 0.5) representation of the Cp ring in the Cp_2V crystal structure at different temperatures for different models of refinement (C = conventional model, TO = two-orientations model).

contribution of the second ring orientation. The in-plane angle of the Cp/Cp* ring rotation at 297 and 357 K is 33.5 and 37.0°, respectively, therefore, it is possible that both approximately eclipsed and staggered molecules are present in the crystal at higher temperature.

The crystal packing of vanadocene is very similar in general features to that for Cp_2Co and Cp_2Ni due to the isomorphous nature and similar behaviour of these crystals. Since the crystal packing of Cp_2Co and Cp_2Ni, as well as of Cp_2Fe, has been discussed and analysed very thoroughly (Antipin, Boese, Augart & Schmidt, 1993; Seiler & Dunitz, 1979*a*, 1980*a*), including very recent atom–atom pairwise potential-energy calculations of crystal packing (Braga & Grepioni, 1992), it is not necessary to discuss this question for vanadocene.

Nevertheless, we should note here that there is in the Cp_2V crystal the same rather short intermolecular contact between two H atoms [atoms H(3) and H(3′) in our setting], related by the inversion centre ($-x$, $-1-y$, $-z$), and the value of this contact is almost unchanged with temperature: 2.48, 2.44 and 2.51 Å at 357, 297 and 170 K, respectively, for TO models, and 2.52 Å at 108 K. The H(3)···H(3′) vector is almost parallel to the *b* axis of the crystal and the above-mentioned negative thermal expansion coefficient for this axis may be related to avoiding the unfavourable H···H interaction on cooling the crystal. All other intermolecular H···H contacts in Cp_2V belonging to the main ring orientation are greater than 2.6–2.7 Å. As found earlier for Cp_2Co, a few contacts of the type H(Cp*)···H(Cp*) were also found in Cp_2V and some of them were too short (1.91–2.15 Å, taking into account the ideal positions of these H atoms in the Cp* rings). This may indicate that a domain-like structure of Cp_2V, suggested earlier for monoclinic ferrocene (Calvarin, Berar & Clec'h, 1982) and cobaltocene (Clec'h & Calvarin, 1985), is questionable in this case.

3.2. *Thermal motion analysis*

The analysis of the atomic anisotropic displacement parameters (ADP's) was made using *THMA*-11 (Trueblood, 1978). The rigid-body LTS tensors for the Cp_2V molecule in the crystal were calculated together with Hirshfeld (Hirshfeld, 1976; Rosenfeld, Trueblood & Dunitz, 1978) quantities $\Delta_{V,C}$ and $\Delta_{C,C}$, in order to estimate the chemical bond rigidity. According to this approach, the value of $\Delta_{A,B}$ is the difference $Z^2_{A,B} - Z^2_{B,A}$, where $Z^2_{A,B}$ is the mean-square vibration amplitude of the *A* atom in the *AB* direction. This rigid-bond test allows one to estimate the quality of the ADP's and the presence/absence of some types of disorder. Some results of the ADP analysis for vanadocene at different temperatures and for different models are summarized in Table 7, where similar data for Cp_2Co, Cp_2Ni, Cp_2Fe and Cp_2Ru are also presented for comparison.

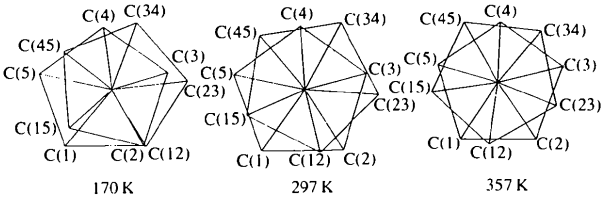

Fig. 2. Schematic representation of the two orientations of the Cp ring in vanadocene at 170, 297 and 357 K.

The best characteristics of the rigid-bond test (mean $\Delta_{C,V}$ and $\Delta_{C,C}$ values) were obtained at 108 K. Compared with the corresponding values for triclinic ferrocene, monoclinic nickelocene and cobaltocene at 100–101 K, these quantities for vanadocene are smallest (Table 7), indicating an ordered structure for Cp_2V at this temperature.

LTS analysis also showed that at 108 K the Cp ring in vanadocene may be regarded as a rigid body. The agreement between experimental U_{ij} values and those calculated from the rigid-body model is characterized by the lowest R' values in the series of the metallocenes studied (in order to avoid the singularities in LTS tensors for cycles, the metal atom was included in this calculation). The corresponding R' values for both C and TO models are much higher at 170 and 297 K. The libration corrections to the C—C and V—C bond lengths are very large at 170 and 297 K (0.02–0.03 and 0.03–0.04 Å, respectively) compared with those at 108 K (0.006–0.008 Å).

The principal eigenvalue $\mathbf{L}_1$ of the libration $\mathbf{L}$ tensor of the Cp_2V molecule at 108 K is equal to 31 deg^2 and the main libration axis is almost parallel to the molecular fivefold axis, as was also found in the crystals of other metallocenes. It is important that this value is smallest when compared with the same values for monoclinic nickelocene and cobaltocene at almost the same temperature and it is very close to that for triclinic ferrocene at 101 K. Much smaller $\mathbf{L}_1$ values for metallocene molecules were found only in orthorhombic ferrocene and ruthenocene (Table 7). The ordered structure of Cp_2V at 108 K provides a very attractive opportunity for an electron-density distribution (EDD) study. Preliminary results of this EDD analysis using the data obtained at 108 K were published by Antipin & Boese (1991) and a paper with the results of the multipole refinement of Cp_2V will be published separately.

Due to a gradual development of the ring disorder at 170 and 297 K, a significant increase in the Hirshfeld's $\Delta_{C,C}$ values was observed, especially for the conventional (C) one-orientation model. For the two-orientation (TO) model these characteristics are much improved. The same trend was also observed for cobaltocene.

The largest eigenvalue of the libration tensor also increases gradually with the temperature, and for vanadocene at 297 K in the C-model approximation $\mathbf{L}_1$ =

Table 7. *Thermal motion analysis data for Cp_2V crystal and some other metallocenes, Cp_2M*

L_1 – The main eigenvalue of the molecular libration tensor (deg^2); B_5-Cp ring rotation barrier from ADP's (kJ mol^{-1}); R' – conventional R' values (%), characterizing the quality of the rigid-body model. All other data are given in Å^2 × 10^4, mean M—C distances (Å) are also given for comparison.

T (K)	$\Delta_{C,M}$	$\Delta_{C,C}$	$\langle\Delta U^2\rangle^{1/2}$	$\langle\sigma(U)^2\rangle^{1/2}$	R'	L_1	M—C	B_5
Vanadocene (this work)								
108	17 (3)	4 (3)	8	3	1.9	31	2.269	8.9 (6)
170	17 (7)	31 (23)	31	8	4.2	82	2.261	—
170*	4 (2)	26 (17)	14	7	3.5	72	2.262	7.1 (8)
297	33 (26)	104 (52)	66	13	6.4	172	2.249	—
297*	30 (14)	56 (55)	20	9	5.3	91	2.259	10.1 (8)
Cobaltocene (Antipin, Boese, Augart & Schmidt, 1993)								
100	20 (12)	44 (43)	45	8	14.9	124	2.097	—
100†	12 (7)	16 (9)	41	5	15.9	91	2.100	—
297	54 (36)	138 (91)	100	23	14.0	247	2.078	—
297†	29 (42)	46 (39)	52	6	9.4	116	2.094	—
Nickelocene (Seiler & Dunitz, 1980*a*)								
101	23 (9)	22 (18)	15	14	7.6	45	2.178	6.5‡
293	—	—	81	36	11.5	199	2.164	5.2
Ferrocene, monoclinic phase (Seiler & Dunitz, 1979*a*)								
173	—	—	—	—	—	231	2.033	2.7
293	—	—	—	—	—	220	2.033	4.7
Ferrocene, triclinic phase (Seiler & Dunitz, 1979*b*)								
101	32–34 (6)	9 (10)	10–12	—	5.9–7.0	28–29	2.046	7.6–12
123	22–26 (8)	—	14–16	—	6.8–7.8	42	2.043	6.4–10.2
148	23–30 (14)	—	20–27	—	7.5–9.9	55–58	2.041	5.9–10
Ferrocene, orthorhombic phase (Seiler & Dunitz, 1982)								
98	—	—	—	—	—	7–9	2.056	23–33
Ruthenocene, orthorhombic phase (Seiler & Dunitz, 1980*b*)								
100	—	—	11	10	10.4	7.3	2.186	>25
293	—	—	23	36	7.5	30.8	2.191	24–38

*Data for the TO model with the occupancy ratios 0.95:0.05 at 170 K and 0.83:0.17 at 297 K. †Occupancy ratios 0.90:0.10 at 100 K and 0.80:0.20 at 297 K. ‡Barriers for nickelocene, ferrocene and ruthenocene were calculated from ADPs by Maverick & Dunitz (1987). For triclinic ferrocene data are given for two independent molecules.

172 deg^2. This very high value hardly describes the real Cp-ring motion and more probably this is a result of the deficiency of the C model used. The corresponding room-temperature data for Cp_2Co, Cp_2Ni and Cp_2Fe are also abnormally high (see Table 7). In the TO-model approximation the L_1 value for Cp_2V decreases almost twice to 91 deg^2, which is more reasonable and is close to the value for Cp_2Co. At 170 K L_1 is 82 and 72 deg^2 for C and TO models, respectively. These intermediate values may be compared only with the data for triclinic ferrocene at 148 K. It is interesting to note that at 173 K in monoclinic ferrocene L_1 = 231 deg^2 (Maverick & Dunitz, 1987), *i.e.* because of the static nature of the ring disorder in Cp_2Fe this value is almost temperature-independent.

It is well known that ADP's obtained from X-ray or neutron diffraction data may be used for a numerical estimation of the slow intramolecular motion characteristics in crystals, in particular rotation barriers for rigid atomic groups (Maverick & Dunitz, 1987; Dunitz, Schomaker & Trueblood, 1988; Dunitz, Maverick & Trueblood, 1988). This approach was used for calculation of ring rotation barriers B_5 in crystals of metallocenes Cp_2Fe, Cp_2Ni, Cp_2Ru (Maverick & Dunitz, 1987; Braga, 1992) and some of their substituted derivatives CpFeCp*, CpRuCp*, Cp^*_2Ru and Cp^*_2Os (Zanin, Antipin & Struchkov, 1990), where Cp* = C_5Me_5 ligand. Good agreement was obtained between B_5 values calculated from ADP's and estimated for the same ligands by other methods, including solid-state NMR, Raman and IR spectroscopies, IQENS and atom–atom potential energy calculations; see the review by Braga (1992).

Our estimation for the Cp-ring rotation barrier B_5 in vanadocene based on the similar ADP analysis (Maverick & Dunitz, 1987), taking into account the second ring orientation, resulted in B_5 values of 8.9 (6) kJ mol^{-1} at 108 K, 7.1 (8) kJ mol^{-1} at 170 K and 10.1 (8) kJ mol^{-1} at 297 K. It is physically unlikely that the barrier increases at the highest temperature, therefore, these data and real errors in B_5 values are probably underestimated. Moreover, the assumption of a B_5 cosine potential may not be strictly appropriate and therefore the values of barriers obtained may be regarded only as some estimations. There is no other experimental data in the literature on the rotation barrier in the vanadocene crystal, but the values obtained are close to those for triclinic ferrocene and are higher than barriers in monoclinic ferrocene

and nickelocene. The largest Cp ring rotation barriers (from ADP's) were found for orthorombic ferrocene and ruthenocene (see Table 7). It should be noted that different spectral data give values of barriers that are very close to those from ADP analysis, namely 5.0–6.3 and 4.4–5.4 kJ mol^{-1} for monoclinic nickelocene and ferrocene, 7.5–11.0 for triclinic ferrocene, 24.8 kJ mol^{-1} for orthorombic ferrocene and 9.6–18.9 kJ mol^{-1} for ruthenocene (Maverick & Dunitz, 1987; Braga, 1992).

4. Summary and concluding remarks

The results of the present multi-temperature study of a vanadocene crystal, together with the structural data for other 3*d*-metallocenes justify the model of a dynamic disorder of the Cp ring with the temperature-dependent gradual appearance in the crystal of the second ring orientation. Two-orientation models have been found to show better agreement for Cp_2V and Cp_2Co than the conventional models, giving more reasonable molecular geometries and ADP characteristics; these models are also compatible with molecular packing analysis. Thus, the nature of the ring disorder in Cp_2V, Cp_2Co and possibly in Cp_2Ni is probably the same. The presence of the second ring orientation is consistent with the appearance of the almost eclipsed molecules that may be obtained by inverting one of the two rings through the centre of symmetry. This interpretation of the disorder in metallocene crystals was first suggested by Seiler & Dunitz (1979*a*), but other interpretations of the disorder, including the presence in the crystal of two orientations of staggered molecules, are also possible.

An important difference between vanadocene, cobaltocene and nickelocene is the totally ordered structure of Cp_2V at 108 K, the main eigenvalue of the libration tensor being the smallest for this molecule. On the contrary, in crystals of Cp_2Ni and Cp_2Co some residual disorder of the Cp-rings still is present at 100 K. Therefore, it is worthwhile to note that in the series of the formally isostructural monoclinic Cp_2M compounds, where M = Fe, Co, Ni and V, a remarkable increase in the M—C distances is observed (from 2.03–2.06 Å for Cp_2Fe to 2.27 Å for Cp_2V), as well as an increase in the corresponding inter-ring distances. This indicates that in the series considered from Cp_2Fe to Cp_2V, the Cp ligands may interpenetrate more towards the metal atom of the neighbouring molecules, thus restricting the ring motions (Braga, 1992). Therefore, a comparison of the values of the B_5 rotation barriers in these compounds, obtained by different methods, as well as a detailed investigation of a possible weak phase transition in the crystal of Cp_2V might be very interesting.

References

Antipin, M. Yu. & Boese, R. (1991). *Proc. Xth Sagamore Conf. on Charge, Spin and Momentum Densities*, p. 4. Konstanz, Germany.

Antipin, M. Yu., Boese, R., Augart, N. & Schmidt, G. (1993). *Struct. Chem.* **4**, 91–101.

Antipin, M. Yu., Lobkovskii, E. B., Semenenko, K. N., Soloveitchik, G. L. & Struchkov, Y. T. (1979). *J. Strukt. Khim. (USSR)*, **20**, 942–944.

Azokpota, C., Pommier, C., Berar, J. F. & Calvarin, G. (1977). *J. Organomet. Chem.* **135**, 125–135.

Braga, D. (1992). *Chem. Rev.* **92**, 633–665.

Braga, D. & Grepioni, F. (1992). *Organometallics*, **11**, 711–718.

Bünder, W. & Weiss, E. (1975*a*). *J. Organomet. Chem.* **92**, 1–6.

Bünder, W. & Weiss, E. (1975*b*). *J. Organomet. Chem.* **92**, 65–68.

Calvarin, G., Berar, J. F. & Clec'h, G. (1982). *J. Phys. Chem. Solids*, **43**, 791–796.

Calvarin, G., Clec'h, G., Berar, J. F. & Andre, D. (1982). *J. Phys. Chem. Solids*, **43**, 785–790.

Campbell, A. J., Fyfe, C. A., Harold-Smith, D. & Jeffrey, K. R. (1976). *Mol. Cryst. Liq. Cryst.* **36**, 1–23.

Clec'h, G. & Calvarin, G. (1985). *Mol. Cryst. Liq. Cryst.* **128**, 305–320.

Cromer, D. T. & Mann, J. B. (1968). *Acta Cryst.* A**24**, 321–324.

Domalski, E. S. & Hearing, E. D. (1990). *J. Phys. Chem. Ref. Data*, **19**, 881–1041.

Dunitz, J. D. & Orgel, L. E. (1953). *Nature (London)*, **171**, 121–122.

Dunitz, J. D. & Seiler, P. (1973). *Acta Cryst.* B**29**, 589–595.

Dunitz, J. D., Maverick, E. F. & Trueblood, K. N. (1988). *Angew. Chem. Int. Ed. Engl.* **27**, 880–895.

Dunitz, J. D., Orgel, L. E. & Rich, A. (1956). *Acta Cryst.* **9**, 373–375.

Dunitz, J. D., Schomaker, V. & Trueblood, K. N. (1988). *J. Phys. Chem.* **82**, 856–867.

Edwards, J. W., Kington, G. L. & Mason, R. (1960). *Trans. Faraday Soc.* **56**, 660–667.

Eiland, P. F. & Pepinsky, R. (1952). *J. Am. Chem. Soc.* **74**, 4971.

Fischer, E. O. & Pfab, W. (1952). *Z. Naturforsch. Teil B*, **7**, 377–379.

Gard, E., Haaland, A., Novak, D. P. & Seip, R. (1975). *J. Organomet. Chem.* **88**, 181–189.

Hirshfeld, F. L. (1976). *Acta Cryst.* A**32**, 239–241.

Kealy, T. J. & Pauson, P. L. (1951). *Nature (London)*, **165**, 1032.

Maverick, E. F. & Dunitz, J. D. (1987). *Mol. Phys.* **62**, 451–459.

Miller, S. A., Tebboth, J. A. & Tremaine, J. F. (1952). *J. Chem. Soc.* pp. 632–636.

Pfab, W. & Fischer, E. O. (1953). *Z. Anorg. Allg. Chem.* **274**, 316–322.

Rogers, R. D., Atwood, J. L., Foust, D. & Rausch, M. D. (1981). *J. Cryst. Mol. Struct.* **11**, 183–188.

Rosenfeld, R. E., Trueblood, K. N. & Dunitz, J. D. (1978). *Acta Cryst.* A**34**, 828–829.

Seiler, P. & Dunitz, J. D. (1979*a*). *Acta Cryst.* B**35**, 1068–1074.

Seiler, P. & Dunitz, J. D. (1979*b*). *Acta Cryst.* B**25**, 2020–2032.

Seiler, P. & Dunitz, J. D. (1980*a*). *Acta Cryst.* B**36**, 2255–2260.

Seiler, P. & Dunitz, J. D. (1980*b*). *Acta Cryst.* B**36**, 2946–2950.
Seiler, P. & Dunitz, J. D. (1982). *Acta Cryst.* B**38**, 1741–1745.
Sheldrick, G. M. (1991). *SHELXTL-Plus*. Release 4.1. Siemens Analytical Instruments Inc., Madison, Wisconsin, USA.
Sourisseau, G., Lucazeau, G., Dianoux, J. J. & Poinsignon, C. (1983). *Mol. Phys.* **48**, 367–377.
Takusagawa, F. & Koetzle, T. F. (1979). *Acta Cryst.* B**35**, 1074–1081.
Trueblood, K. N. (1978). *Acta Cryst.* A**34**, 950–954.
Weiss, E. & Fischer, E. O. (1955). *Z. Anorg. Allg. Chem.* **278**, 219.
Wilkinson, G., Rosenblum, M., Whiting, M. C. & Woodward, R. B. (1952). *J. Am. Chem. Soc.* **74**, 2125.
Willis, B. T. M. (1960). *Acta Cryst.* **13**, 763–776.
Wong, C., Lee, T. Y., Chao, K. J. & Lee, S. (1972). *Acta Cryst.* B**28**, 1662–1665.
Zanin, I. E., Antipin, M. Yu. & Struchkov, Yu. T. (1990). *Acta Cryst.* A**46**, C-299.